ILIA International Information and Engineering Technology Association

International Journal of Heat and Technology

Vol. 43, No. 2, April, 2025, pp. 751-759

Journal homepage: http://iieta.org/journals/ijht

Energy Balance Sheet of Blends of Jatropha Biodiesel at Variable Injection Hole Number in a Single-Cylinder Diesel Engine-An Experimental Approach



Surya Prasad Adhikari ^{1*}, Rupesh Lal Karn², Sangam Bhusal², Laxman Palikhel², Saurabha Bhattarai ³

- ¹ Department of Mechanical and Aerospace Engineering, Pulchowk Campus, Institute of Engineering, Tribhuvan University, Kirtipur 44101, Nepal
- ² Department of Automobile and Mechanical Engineering, Thapathali Campus, Institute of Engineering, Tribhuvan University, Kirtipur 44600, Nepal
- ³ Forest Bio-material Science and Engineering, Madan Bhandari University, Chitlang 44100, Nepal

Corresponding Author Email: spadhikari@pcampus.edu.np

Copyright: ©2025 The authors. This article is published by IIETA and is licensed under the CC BY 4.0 license (http://creativecommons.org/licenses/by/4.0/).

https://doi.org/10.18280/ijht.430234

Received: 27 December 2024 Revised: 6 April 2025 Accepted: 21 April 2025

Available online: 30 April 2025

Keywords:

thermodynamics first law, heat equivalent to brake power, blends of Jatropha biodiesel, exhaust gas temperature

ABSTRACT

This study investigates the thermal performance and emission characteristics of a singlecylinder, water-cooled diesel engine using Jatropha biodiesel (JB) blends (5 JB, 10 JB, 20 JB) and conventional diesel fuel. Experiments were conducted under varying injector configurations (3-hole, 4-hole, 5-hole) and operational loads (10-100%) using an eddy current dynamometer. A detailed thermodynamic energy balance was performed, accounting for Heat Equivalent to Brake Power (HBP), Heat in Jacket Cooling Water (HJW), Heat in Exhaust Gases (HGas), and Heat Radiation (HRad). Results revealed that the 3-hole injector configuration delivered the highest thermal efficiency, achieving peak HBP values of 25.68% for diesel and 26.01% for the 5 JB blend at 70% load, along with the lowest exhaust gas temperatures (EGT) and minimal radiative losses. In contrast, the 4-hole and 5-hole injectors showed higher cooling losses (HJW up to 55.22%) and radiative dissipation (HRad up to 53.48% for 20 JB), with significantly elevated EGTs (up to 471.94°C for the 5-hole configuration), which correlated with increased nitrogen oxide (NO) emissions. Biodiesel blends effectively reduced carbon monoxide (CO) and carbon dioxide (CO₂) emissions by 19.28% and 13.25%, respectively, although NO emissions rose by 31.32% at higher blend ratios. Overall, the 3-hole injector offered the best balance between energy efficiency and emission control, with the 5 JB blend demonstrating performance metrics closely comparable to diesel.

1. INTRODUCTION

The heat generated inside the combustion chamber is transferred to the cylinder wall and exhaust system through radiation. As the crankshaft rotates, the geometry of the flow system becomes irregular and changes periodically. Heat flows along the cylinder walls from hotter to cooler areas. The heat generated inside the combustion chamber from fuel burning is divided into four parts. They are heat equivalent to brake power, heat loss in jacket cooling water, heat loss in gases, and heat loss due to radiation. Generally, heat loss due to radiation is also referred to as unaccounted heat. Heat equivalent to brake power is referred to as useful work related to the brake thermal efficiency. Heat in jacket cooling water refers to the heat transmitted to the coolant [1].

The injector hole diameter and the number of injector holes (IHN) significantly influence engine performance, combustion efficiency, and emission characteristics. These parameters are crucial in determining the size of fuel droplets, the penetration depth of the fuel spray, and the overall quality of fuel atomization [2, 3]. Spray angle, spray tip penetration, and nozzle area significantly influence fuel atomization and the

swirl intensity of the air-fuel mixture, which in turn affect the performance, combustion characteristics, and emission profile of diesel engines [4]. Smaller hole diameters and a higher number of holes typically produce finer fuel droplets, enhancing atomization and promoting better air-fuel mixing. This improved mixing leads to more efficient and complete combustion, resulting in higher thermal efficiency and reduced emissions of unburned hydrocarbons (HC) and CO [5]. Conversely, suboptimal injector configurations can lead to poor atomization, larger droplet sizes, and inadequate penetration, which may cause incomplete combustion, increased fuel consumption, and elevated levels of harmful emissions such as particulate matter and nitrogen oxides (NOx). Therefore, optimizing both the diameter and number of injector holes is essential for improving combustion dynamics and achieving a desirable balance between engine performance and environmental impact [6]. An increase in the number of injector holes beyond an optimal threshold can have a detrimental impact on engine combustion and emission characteristics. While a moderate rise in injector hole number generally improves fuel atomization and spray dispersion, excessive hole numbers can lead to unfavorable combustion behavior. This is primarily due to insufficient air entrainment, which disrupts the formation of a proper stoichiometric airfuel mixture [7]. With more holes, the fuel is injected in multiple, smaller streams that may not adequately penetrate the combustion chamber, especially in compact or low-swirl environments. As a result, the fuel may not mix uniformly with the available air, leading to localized fuel-rich zones and incomplete combustion. This imbalance can cause increased emissions of CO, unburned HC, and particulate matter (PM), while also potentially raising NOx emissions due to higher peak local temperatures in fuel-rich regions [8]. Therefore, careful optimization of the injector hole number is crucial to maintain an effective air-fuel ratio, ensure complete combustion, and minimize pollutant formation.

Montgomery et al. [9] investigated the effect of injector nozzle hole size (225 µm, 260 µm, and 300 µm) and number (6 and 8) of a heavy-duty diesel engine when fueled with pure diesel. The results indicated that the injector configuration with the fewest number of holes and the smallest hole diameter the most favorable emission performance, significantly reducing pollutants such as CO, HC, and PM. Additionally, this configuration achieved the second-best brake-specific fuel consumption (BSFC), demonstrating a commendable balance between fuel efficiency and emission control. Yoon et al. [4] investigated the effect of swirl ratio and injector hole number (7, 8, 9, and 10) on the combustion and emission characteristics of a light-duty diesel engine. The results indicated that increasing the number of injector holes led to a reduction in PM and CO emissions, but caused an increase in NOx emissions. Mohiuddin et al. studied the effect of injector hole number on engine performance in a light-duty diesel engine by varying the injector number from 7 to 10. The results showed that increasing the number of injector holes reduced the ignition delay [10].

Dong et al. [11] investigated the effect of IHN on combustion and emission characteristics of ethanol/diesel dual-fuel engines keeping the total orifice area and spray angle the same, where the swirl ratio is 1.85, the compression ratio is 17.3:1 and the IHN varies from 4 to 8. The findings indicated that as the number of IHN increased, both the in-cylinder peak pressure and the rate of pressure rise also showed a significant increase. On the other hand, when the number of nozzle holes was reduced, a noticeable decrease in NOx emissions was observed. This reduction is likely due to lower combustion temperatures associated with slower and less intense burning. However, this came at the cost of a slight increase in soot emissions, likely resulting from incomplete combustion and reduced oxygen availability in localized zones. Therefore, merely modifying the combustion design parameters of the engine is insufficient to significantly improve its performance and reduce emissions. As a result, researchers are increasingly exploring alternative fuels that have the potential to enhance the performance characteristics of internal combustion (IC) engines while simultaneously minimizing exhaust emissions.

Blends of non-edible oils, such as Jatropha oil biodiesel, have been identified as viable alternatives to conventional diesel fuel for use in IC engines. One of the key advantages of Jatropha biodiesel is that it can be blended with diesel and utilized without requiring any significant modifications to the engine. This makes it a practical and cost-effective renewable fuel option. However, experimental investigations have shown that when Jatropha biodiesel-diesel blends are used, the brake thermal efficiency (BTE) of the engine tends to be lower compared to that of pure diesel. Additionally, brake-specific

fuel consumption (BSFC) was found to be higher for the biodiesel blends, indicating that a greater quantity of fuel is required to produce the same amount of power [12, 13]. Consequently, a series of experimental investigations were conducted to evaluate the performance, combustion behavior, and emission characteristics of Jatropha oil blends when utilized as fuel in compression ignition (CI) engines. These studies aimed to assess the feasibility of using Jatropha oil as an alternative fuel by analyzing its impact on engine efficiency, combustion quality, and exhaust emissions under various operating conditions.

Chauhan et al. [12] found that Jatropha biodiesel blends exhibit lower peak cylinder pressure and shorter ignition delay compared to conventional diesel. Additionally, these blends demonstrated reduced BTE, primarily due to their lower calorific value. The studies also reported higher BSFC and lower EGT in comparison to diesel. While CO emissions were lower for all Jatropha blends, NOx emissions increased as the blending ratio and engine load rose [14]. Agarwal and Agarwal [15] demonstrated that Jatropha oil blends with diesel up to 20% exhibit performance and combustion characteristics comparable to pure diesel. These blends result in lower CO and HC emissions compared to diesel; however, NOx emissions are higher. Further investigation into diesel engine performance revealed that engines can operate effectively with Jatropha blends without the need for any modifications [16].

Mofijur et al. [17] conducted a study on the performance of Jatropha blends in a single-cylinder CI engine and found that as the blending ratio of Jatropha with diesel increased, brake power decreased while specific fuel consumption rose. At a 20% Jatropha blend, CO and HC emissions were lower compared to pure diesel. However, NOx emissions showed a slight increase in this blending ratio.

Bhatta et al. [18] conducted a comprehensive investigation into the performance, combustion, and emissions of the Jatropha biodiesel blend where trans-esterified Jatropha oil was preheated to 100°C before being mixed with diesel. They found that blends containing up to 20% JB exhibited engine performance and combustion characteristics comparable to pure diesel. Blends exceeding the 20% threshold demonstrated significantly greater engine performance and combustion behavior deviations.

Palash et al. [19] investigated the effect of adding the antioxidant N, N0 -diphenyl1, 4-phenylenediamine (DPPD) on NOx emissions in CI engines fueled by JB blends. Their findings revealed that while the addition of DPPD effectively reduced NOx emissions, it also led to a significant reduction in BP and a slight increase in specific fuel consumption (SFC). Adding 0.15% DPPD to Jatropha blends resulted in a reduction of NOx emissions by 8.03%, 3.50%, 13.65%, and 16.54% for 5 JB, 10 JB, 15 JB, and 20 JB, respectively. Additionally, the study found that HC and CO emissions were lower for all Jatropha blends compared to pure diesel.

A comprehensive literature review reveals that Jatropha, a non-edible oilseed with high recovery rates after transesterification, shows significant promise as an alternative fuel for CI engines when blended with biodiesel. Due to its advantageous fuel properties, JB blends have the potential to serve as a viable substitute for conventional diesel. However, one of the main challenges associated with using Jatropha blends in CI engines is the increased NOx emissions compared to pure diesel. To address this issue, several strategies can be implemented, including the addition of oxidants, adjustment of injection timing, or pre-heating the Jatropha blends before

injection into the engine. These methods can help optimize combustion conditions and reduce NOx formation.

While JB blends demonstrate considerable potential as an alternative fuel, the impact of varying operational parameters, such as the IHN, on engine performance, combustion, and emissions has not been thoroughly investigated. Although there is a growing body of research on the performance of biodiesel blends in CI engines, a notable gap exists in understanding the thermodynamic behavior resulting from these variations. This gap presents an opportunity for further exploration. The current research aims to address this by examining the thermodynamic and emission characteristics of CI engines when the IHN and biodiesel blending ratios are varied. The study will be conducted using an eddy current dynamometer, with the engine operating at a constant RPM, to provide a more comprehensive understanding of the effects of these parameters.

2. MATERIAL AND METHOD

2.1 Oil production

The crude Jatropha oil was provided by the Alternative Energy Promotion Center (AEPC), Baneshowor, Kathmandu, Nepal and transesterification is performed at the Nepal Academy of Science and Technology, Khumaltar, Lalitpur, Nepal.

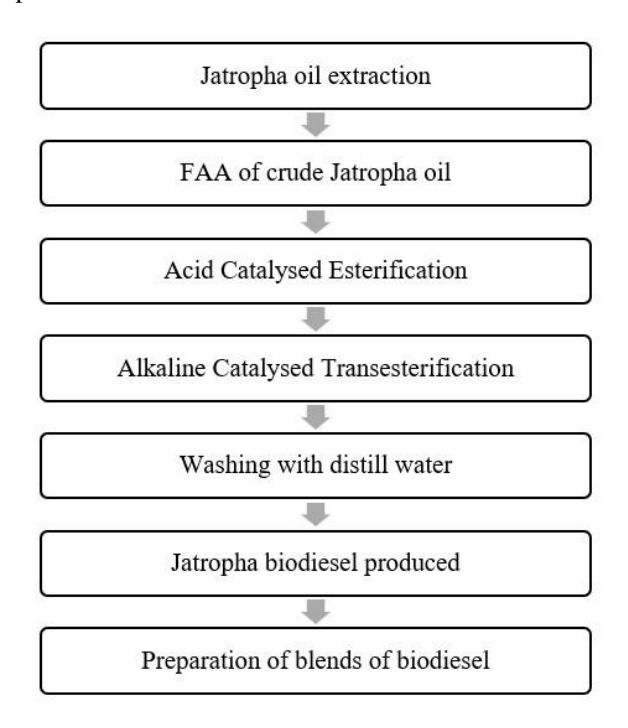


Figure 1. Biodiesel blend preparation procedures

Table 1. Steps for biodiesel production

Step	Types of Esterification	Reagent Used
1	Acid-Catalyzed Esterification	Blend of 30% w/w methanol to oil and 0.75 w/w concentrated H ₂ SO ₄
2	Alkaline Catalyzed Transesterification	20% methanol and 1.5% KOH w/w ratios to oil

2.2 Test method

2.2.1 Research engine

The test was carried out on a single-cylinder diesel engine by varying the injector hole number. The 3-hole (3-IHN), 4-hole (4-IHN), and 5-hole (5-IHN) injectors were used and the engine was run at a steady speed of 1500 rpm with a compression ratio of 17.5.

The engine specifications are given in Table 2.

Table 2. Test engine specifications

Parameters	Specifications					
Bore	87.55 mm					
Stroke length	110 mm					
Rated power	3.5 kW					
Rated speed	1500 RPM					
Connecting rod length	234 mm					
Swept Volume	661.45 cc					
Torque	11.5 Nm					
Injection Timing	23° before TDC					
Type of Loading	Eddy current dynamometer					
Load cell	Strain gauge, range 0-50 kg					
Load indicator	Digital, range 0-50 kg, supply 220 V					
Temperature sensor	RTD, PT 100 and Thermocouple, type K					
Orifice diameter	20 mm					
Piezo sensor	Range 5000 Psi, low noise cable					
Pressure sensor range	0-350 bar					

Combustion parameters:

Air density (kg/m³): 1.17
Polytrophic index: 1.12
Adiabatic index: 1.41
Number of cycles: 10

Smoothing 2TDC reference: 0

• Cylinder pressure reference: 1

Performance parameters:

Orifice diameter (mm): 20.00
Pulses per revolution: 360

• Dynamometer arm length (mm): 185

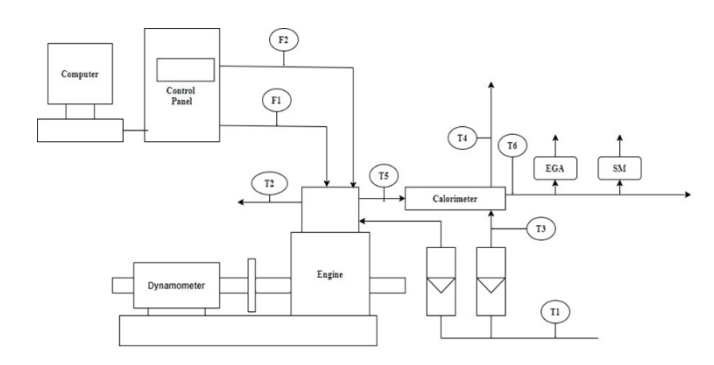


Figure 2. Schematic diagram of VCR engine

F1 = Fuel consumption (kg/hr)

F2 = Air consumption (kg/hr)

F3 = Jacket cooling water (kg/hr)

F4 = Calorimeter water flow (kg/hr)

T1 =Jacket water inlet temp (°C)

T2 = Jacket water outlet temp (°C)

T3 = Calorimeter water inlet temp (°C)

T4 = Calorimeter water outlet temp (°C)

T5 = Exhaust gas to calorimeter inlet temp (°C)

T6 = Exhaust gas from calorimeter outlet temp (°C)

2.2.2 Gas analyzer

The KANE Model: AUTO5-2 exhaust gas analyzer was used to measure the emission characteristics. The analyzer specifications are illustrated in Table 3.

Table 3. Specification of gas analyzer

Parameter	Resolution	Accuracy	Range	
Carbon Monoxide (Infrared)	0.01%	+/- 5% of reading +/- 0.06% volume	0-10% Over-range 20%	
Carbon Dioxide (Infrared))	0.1%	+/- 5% of reading +/- 0.5% volume	0-16% Over- range: 25%	
Nitric Oxide (Fuel cell)	1 ppm	0-1500 ppm +/- 5% or 25 ppm;	0-1500 ppm Over- range: 5000 ppm	

2.3 Related theory

The general approach to the thermal balance of an IC engine is based on the first law of thermodynamics applied to a control volume. From thermodynamics' first law, according to the conservation of energy.

$$Q_s = Q_b + Q_w + Q_{ex} + Q_{rad} \tag{1}$$

where

 Q_s = heat supplied by burning of fuel

 Q_b = heat equivalent to brake power

Qw = heat lost in jacket cooling water

 Q_{ex} = heat loss in exhaust

 Q_{rad} = heat loss due to radiation

Heat loss due to radiation is often termed as heat loss due to miscellaneous or unaccounted heat.

Heat supplied by the burning of fuel is calculated by:

$$O_s = M_f * C_{vf}$$
 (2)

where,

 $M_{\rm f}$ = mass of fuel flow rate

 C_{vf} = Calorific value of fuel

The heat equivalent to brake power is referred to as brake power (BP) and it is calculated by:

$$BP = 2*\pi*N*T \tag{3}$$

where,

N = speed of crankshaft

T= Torque offered by the engine

Heat lost in jacket cooling water (Q_w) is the heat that is taken away by cooling water and is calculated by:

$$Q_{w} = m_{w} * C_{vW} * \Delta T_{w}$$
 (4)

where.

 $m_w = mass flow rate of water$

C_{Vw} = calorific value of water

 ΔT_w = change in temperature of a calorimeter, (T_2-T_1)

There are two ways to calculate heat loss in exhaust.

One is by considering the average specific heat (Cg) of gases at the mean exhaust temperature [4].

$$Q_{ex} = (m_f + m_a) * C_g * (Tg - T_a)$$
 (5)

where.

 $m_a = mass of air$

 C_g = specific heat of gas

Another method is using an exhaust calorimeter [5, 6], where $Q_{\rm ex}$ is calculated by:

$$Q_{ex} = m_w * C_w * \Delta T_w + (m_f + m_a) * C_p * T_{cl}$$
 (6)

whore

 C_w = specific heat of water

Unaccounted heat or heat due to radiation is calculated by subtraction:

$$Q_{rad} = Q_s - Q_b - Q_w - Q_{ex}$$
 (7)

3. RESULTS

Table 4 presents the fuel properties of pure JB and a 20% JB blend. The results show that pure JB has higher density, viscosity, and flash point, which may negatively affect fuel atomization and spray penetration in a diesel engine. However, pure Jatropha biodiesel also has a lower calorific value, leading to reduced heat content in the engine. As a result, it is not suitable as a direct substitute for conventional diesel in CI engines. In contrast, the 20% Jatropha biodiesel blend exhibits improved fuel properties compared to pure Jatropha biodiesel.

Table 4. Fuel property

Fuel Property	Pure Jatropha	20 JB	Diesel	Test Method	
Density (kg/m³)	875	843	835	ASTM D 4052	
Kinematic viscosity (CST)	5.72	2.939	2.42	ASTM D 445	
Cetane number	53	55	51	ASTM D 613 2006	
Flashpoint (°C)	64	45	42	ASTM D 93 2018	
Calorific value (KJ/KG)	39500	42500	44000	Bomb Calorimeter	

Figure 3 illustrates the fuel flow rates for different IHN across various blends of Jatropha biodiesel. The results indicate that the fuel consumption for the 5-IHN configuration was higher compared to 4-IHN and 3-IHN. Additionally, diesel exhibited a lower fuel flow rate than all biodiesel blends, irrespective of the injector hole number. An increase in the biodiesel blending ratio corresponded with a rise in fuel flow rate.

Compared to diesel, the fuel flow rate for 5 JB, 10 JB, and 20 JB increased by 0.62%, 4.99%, and 5.47% respectively for the 3-IHN configuration; by 1.47%, 2.82%, and 4.38% for 4-IHN; and by 2.80%, 6.70%, and 9.85% for 5-IHN. This progressive increase in fuel flow rate can be attributed to the higher density and viscosity of JB relative to conventional

diesel. As the blending ratio of biodiesel increased, these physical properties became more pronounced, resulting in higher fuel consumption. The elevated viscosity and density affected the atomization process and air-fuel mixing, ultimately influencing the combustion characteristics and efficiency of the engine [20].

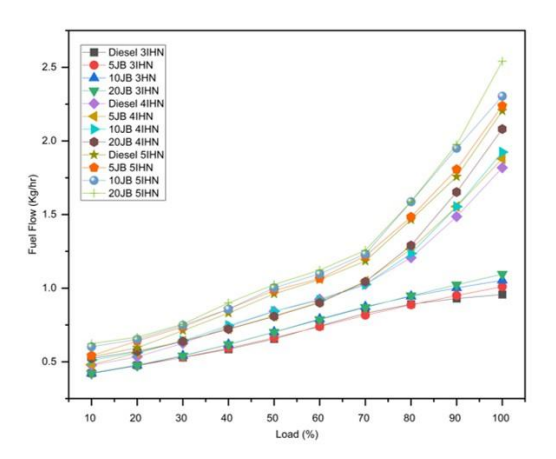


Figure 3. Relation of fuel flow rate with load for various IHN

A diesel engine operating at a constant speed with a variable compression ratio (VCR) was used to test the fuel samples. Table 5 presents the thermal balance sheet for JB blends and pure diesel. The results indicate that the 3-IHN configuration consistently exhibited the highest heat utilization in HBP, regardless of the fuel blend or load applied. The remaining heat was dissipated as losses through jacket cooling water, exhaust gases, and radiation. Heat loss through jacket cooling water was greater in the 3-IHN configuration compared to 4-IHN and 5-IHN. Conversely, EG heat loss was highest in 5-IHN, followed by 4-IHN and then 3-IHN. This increased exhaust gas heat loss in higher-IHN configurations is a key factor contributing to elevated NOx emissions.

Figure 4 illustrates the effect of heat equivalent to brake power (HBP) across different IHN, considering various JB biodiesel blend ratios under multiple load conditions. The results show that increasing the IHN leads to a reduction in the proportion of heat converted into useful work, as indicated by the HBP values. Furthermore, a consistent decrease in HBP was observed with higher biodiesel blending ratios, regardless

of the injector hole configuration. This reduction in HBP is primarily attributed to the lower calorific value of JB compared to conventional diesel, which results in less energy being available for conversion into mechanical output [21].

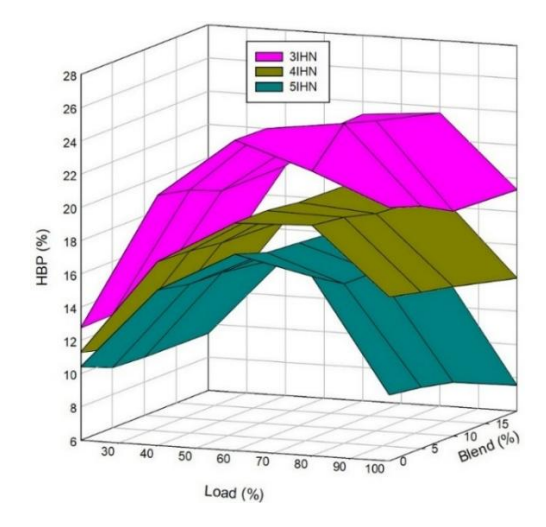


Figure 4. Relation of HBP for various blend ratio biodiesel at various injection hole numbers

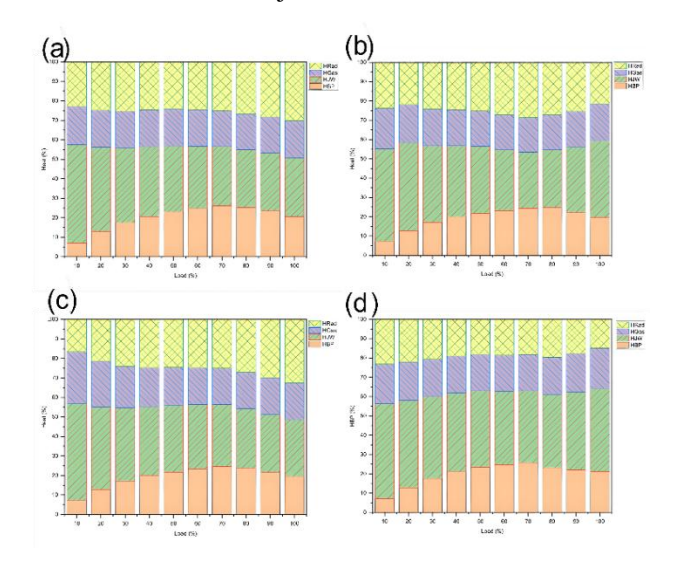


Figure 5. Thermal balance of 5 JB (a), 10 JB (b), 20 JB (c) and pure diesel (d) for 3-IHN

Table 5. Thermal balance sheet of JB blends and diesel

		3-Hole			4-Hole				5-Hole				
Sample	Load (%)	HBP (%) H	TT TXX/ (0/)	IICon (0/)	HRad (%)	HBP	HJW	HGas	HRad	HBP	HJW	HGas	HRad
			113 W (70)	HGas (70)		(%)	(%)	(%)	(%)	(%)	(%)	(%)	(%)
5 JB	20	12.80	43.43	18.99	24.77	10.75	41.79	28.09	19.37	9.62	41.56	32.36	16.46
	50	22.91	33.93	19.06	24.10	18.67	30.90	23.46	26.98	16.24	30.09	25.43	28.25
	80	25.23	29.75	18.27	26.74	19.59	22.22	20.65	37.54	15.59	29.21	22.64	32.56
	100	20.56	30.28	19.00	30.17	15.39	15.35	16.44	52.82	9.67	28.40	20.00	41.93
10 JB	20	12.79	45.62	19.79	21.80	10.66	41.54	24.46	23.33	9.50	40.08	26.55	23.88
	50	21.65	34.82	18.39	25.13	18.04	30.75	23.10	28.11	16.99	16.01	33.40	25.22
	80	24.65	30.04	18.11	27.20	19.07	22.28	20.67	37.98	15.57	25.17	21.74	37.51
	100	19.52	39.79	19.22	12.47	14.98	16.44	16.99	51.59	9.23	22.60	19.70	48.48
20 JB	20.00	12.81	42.39	23.45	21.33	10.61	43.15	25.12	21.13	9.44	44.07	25.70	20.79
	50.00	21.69	34.43	19.33	24.55	18.02	29.89	22.61	29.48	15.43	34.31	24.02	26.23
	80.00	23.62	30.71	18.60	27.07	18.72	23.73	20.11	37.44	14.33	30.01	20.66	35.01
	100.0	19.31	29.24	18.92	35.53	13.99	15.90	16.63	53.48	7.54	26.06	17.32	49.07
Diesel	20.00	12.75	45.27	19.89	22.09	11.29	41.59	25.13	21.98	10.42	40.34	27.50	21.74
	50.00	23.38	39.67	18.79	18.16	18.74	24.00	22.02	35.23	16.99	28.93	23.42	30.66
	80.00	23.12	38.07	19.21	19.61	19.86	18.26	19.99	41.89	16.78	23.16	20.18	39.87
	100.0	21.24	43.02	20.83	14.91	15.86	13.44	15.49	9.97	24.49	18.66	46.88	9.97

Figure 5 illustrates the distribution of heat at varying load percentages for different blend ratios of JB (5 JB, 10 JB, 20 JB) and pure diesel using the 3-IHN configuration. For diesel, the HBP increases progressively from 7.01% at 10% load to a peak of 25.68% at 70% load, followed by a slight decline to 21.24% at full load. A similar trend is observed for the 5 JB blend, which reaches a maximum HBP of 26.01% at 70% load before decreasing to 20.56% at 100% load. The 10 JB blend peaks at 24.33% HBP at 70% load, while the 20 JB blend shows a continuous rise, achieving a maximum HBP of 19.31% at full load.

HJW for diesel begins at 49.28% at 10% load and gradually decreases to 43.02% at full load. The 5 JB blend records a slightly higher initial HJW (50.45% at 10% load), which aligns more closely with diesel at higher loads, dropping to 30.27% at full load. The 10 JB and 20 JB blends follow a similar pattern, with 10 JB decreasing from 48.27% to 39.79%, and 20 JB from 49.88% to 29.24% as load increases.

HGas for diesel remains relatively stable, ranging between 18.66% and 20.83%. HRad, however, declines from 23.10% at 10% load to 14.91% at full load for diesel. Biodiesel blends show comparable HGas values but exhibit higher HRad, particularly at higher loads, for instance, 20 JB records an HRad of 32.53% at 100% load, indicating increased unutilized heat loss at full engine load.

Figure 6 illustrates the heat distribution at varying load percentages for different blend ratios of JB (5 JB, 10 JB, 20 JB) and pure diesel using the 4-IHN configuration. For diesel, the HBP increases from 6.18% at 10% load to a peak of 20.20% at 70% load, before declining to 15.86% at full load. The 5 JB blend follows a similar pattern, peaking at 17.46% HBP at 70% load, then dropping to 6.97% at 100% load. Both the 10 JB and 20 JB blends exhibit lower HBP values, with 20 JB reaching 13.99% HBP at full load.

HJW for diesel decreases sharply from 45.27% at 10% load to 13.44% at full load. The 5 JB blend also shows a reduction, from 48.59% to 28.40%, while 20 JB experiences the most significant decrease, from 46.43% to 15.90%.

For HGas, diesel shows a decline from 25.92% at 10% load to 15.49% at full load. The 20 JB blend follows a similar trend, decreasing from 26.13% to 16.63%. However, HRad rises significantly for all fuels, with diesel reaching 55.22% and 20 JB recording 53.48% at full load.

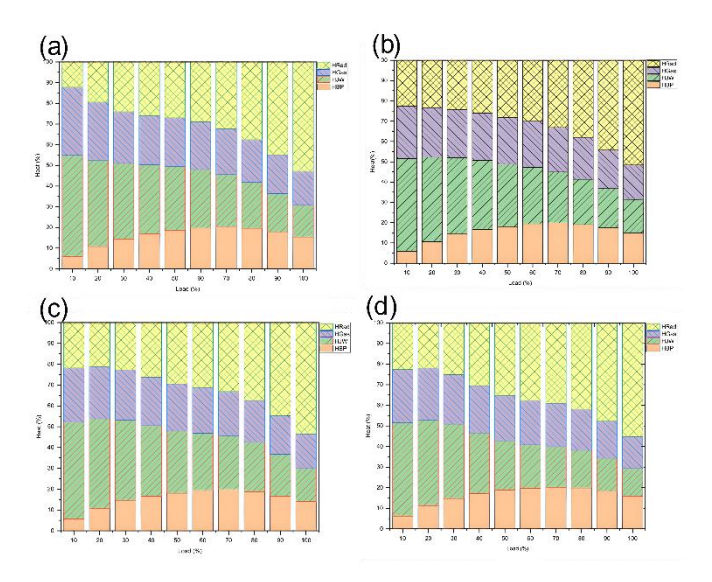


Figure 6. Thermal balance of 5 JB (a), 10 JB (b), 20 JB (c) and pure diesel (d) for 4-IHN

Figure 7 illustrates the heat distribution at varying load percentages for different JB blend ratios (5 JB, 10 JB, 20 JB) and pure diesel using the 5-IHN configuration. The 5-IHN configuration yields the lowest HBP values. For diesel, HBP increases from 5.67% at 10% load to 17.81% at 60% load, before declining to 9.97% at full load. The 5 JB blend peaks at 17.15% HBP at 60% load, then decreases to 6.97% at full load. The 20 JB blend reaches a maximum of 7.54% HBP at full load.

HJW for diesel starts at 43.81% at 10% load and decreases to 24.49% at full load. The 5 JB blend shows a reduction from 48.59% to 28.40%, while the 20 JB blend decreases from 45.23% to 24.49%.

HGas for biodiesel blends is higher at low loads, with 5 JB exhibiting 39.21% at 10% load, but declines at higher loads, reaching 20.00% at full load. HRad increases significantly across all fuels, with diesel reaching 46.88% and 5 JB achieving 41.93% at full load.

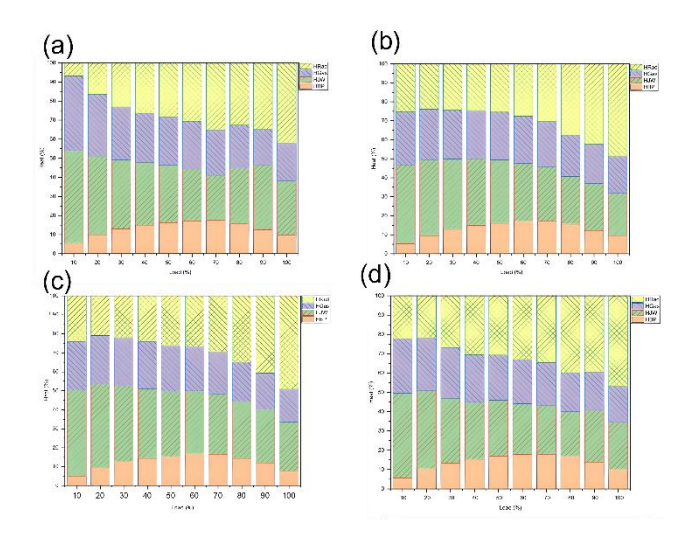


Figure 7. Thermal balance of 5 JB (a), 10 JB (b), 20 JB (c) and pure diesel (d) for 4-IHN

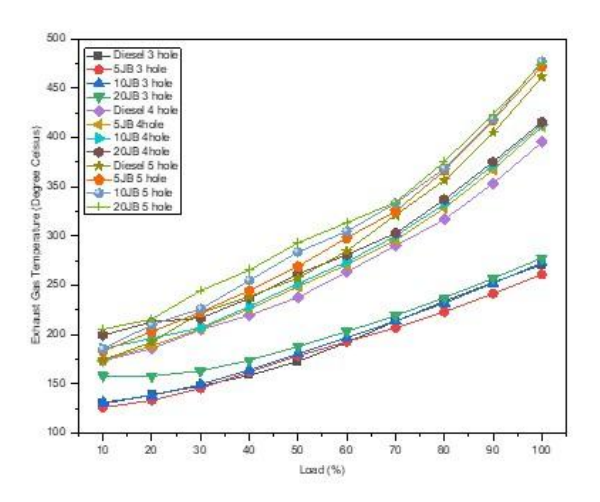


Figure 8. Relation of exhaust gas temperature with load for various IHN

Figure 8 illustrates the EGT for various blends of JB and diesel fuel across different injector hole numbers (3-IHN, 4-IHN, and 5-IHN). Among the configurations, 5-IHN consistently shows the highest EGT values, followed by 4-IHN and 3-IHN.

For the 3-IHN configuration, the EGT ranges from 125.66°C to 261.07°C for 5 JB, 130.84°C to 272.73°C for 10 JB, 158.10°C to 277.64°C for 20 JB, and 129.69°C to 270.90°C for pure diesel. Under 4-IHN, the EGT values increase, ranging from 173.78°C to 411.19°C for 5 JB, 185.60°C to 413.06°C for 10 JB, 199.27°C to 415.73°C for 20 JB, and 173.14°C to 395.23°C for diesel. For the 5-IHN configuration, the highest temperatures are observed: 183.12°C to 471.94°C for 5 JB, 185.24°C to 477.10°C for 10 JB, 205.29°C to 474.92°C for 20 JB, and 173.90°C to 461.53°C for diesel.

A comparative analysis of diesel shows that, for 3-IHN, the EGT of 5 JB is 1.90% lower, while 10 JB and 20 JB are 1.18% and 7.84% higher, respectively. For the 4-IHN configuration, EGT increases by 3.23%, 5.55%, and 9.25% for 5 JB, 10 JB, and 20 JB, respectively, compared to diesel. A similar trend is observed in 5-IHN, where EGT increases by the same percentages for the respective blends.

The data indicate that EGT rises with both the increase in injector hole number and the biodiesel blending ratio. This rise is attributed to greater combustion intensity and increased heat loss through exhaust gases, particularly in the 4-IHN and 5-IHN configurations [22].

Figure 9 illustrates the emission characteristics of various JB blends using 3-IHN, 4-IHN, and 5-IHN injectors, detailing CO (Figure 9(a), CO₂ (Figure 9(b)), and NO (Figure 9(c)) emissions. As biodiesel contains oxygen and has a lower carbon content compared to conventional diesel, it contributes to reduced CO and CO₂ emissions. The results show that increasing the biodiesel blending ratio leads to a noticeable decrease in CO and CO₂ emissions, while NO emissions tend to increase.

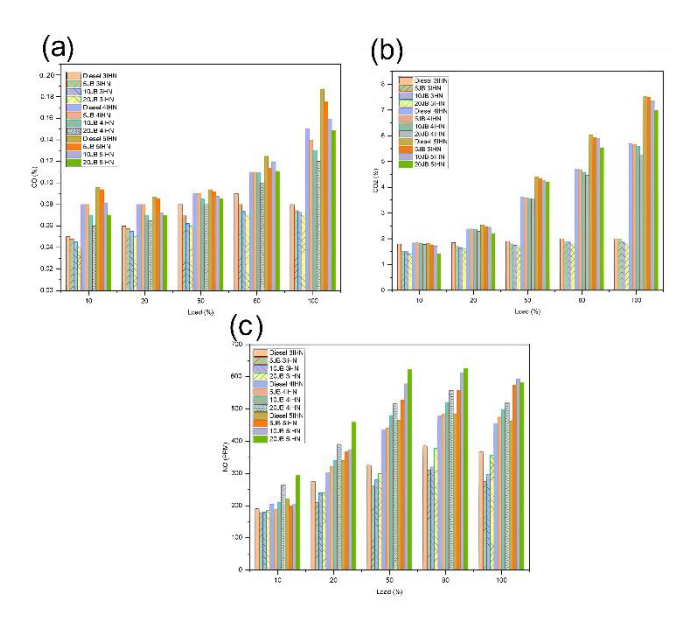


Figure 9. Relation emissions with load for various IHN (a) CO, (b) CO₂, and (c) NO

Additionally, an increase in the number of injector holes is associated with higher emissions of CO, CO₂, and NO. This is largely due to the improved atomization and better fuel-air mixing provided by injectors with more holes, which enhances combustion efficiency. The rise in NO emissions is primarily attributed to the elevated in-cylinder and exhaust gas temperatures that result from more complete and intense combustion, a condition favorable for NO formation. Similarly, the increase in CO₂ emissions can be attributed to

the higher volume of fuel injected through higher-hole injectors. This promotes more complete oxidation of the fuel, thereby increasing CO₂ levels as a byproduct of efficient combustion [23].

A comparative analysis with diesel for the 3-IHN configuration shows that CO emissions decrease by 7.90%, 13.54%, and 19.28% for 5 JB, 10 JB, and 20 JB blends, respectively. For 4-IHN, the reductions are slightly lower at 1.33%, 8.78%, and 16.79%, while for 5-IHN, CO emissions are reduced by 4.36%, 11.61%, and 17.41% for the respective blends.

Similarly, CO_2 emissions also show a declining trend with increasing biodiesel content. Compared to diesel in the 3-IHN setup, CO_2 emissions decreased by 7.00%, 9.07%, and 13.25% for 5 JB, 10 JB, and 20 JB, respectively. Under the 4-IHN configuration, the reductions are more modest at 0.54%, 1.53%, and 4.32%, while for 5-IHN, they stand at 2.14%, 3.35%, and 11.25%.

In contrast, NO emissions exhibit an upward trend with higher biodiesel blending ratios. For 3-IHN, NO emissions increase by 6.94%, 17.00%, and 24.14% for 5 JB, 10 JB, and 20 JB, respectively. Under 4-IHN, the increases are 0.76%, 8.55%, and 21.38%, while the 5-IHN configuration shows the highest rise at 10.07%, 16.27%, and 31.32% for the respective blends.

These trends highlight the oxygen-rich nature of biodiesel, which enhances combustion efficiency and reduces CO and CO₂ emissions, while also raising combustion temperatures that promote NO formation.

4. DISCUSSION

The influence of varying injector hole numbers on engine performance and emissions is evident from the experimental results. As the number of injector holes increases, a corresponding rise in fuel consumption is observed, primarily due to enhanced fuel delivery and atomization. Despite this increase, the test engine, a constant-speed diesel engine coupled with an eddy current dynamometer, demonstrates a linear increase in BP as the applied load increases.

Notably, the BP output remains relatively consistent across all biodiesel blends and injector configurations at corresponding load conditions. This suggests that while injector hole number and fuel type affect fuel flow and combustion characteristics, they do not significantly alter the engine's ability to produce power under steady operating conditions.

An intriguing observation emerges when examining the different injector configurations in detail. The heat balance percentage (%HBP) for the 3-IHN is consistently higher than that of the 4-IHN and 5-IHNs, indicating a more efficient conversion of the supplied thermal energy into useful brake power. This suggests that the 3-IHN promotes more effective combustion and energy utilization under the tested conditions.

In contrast, the 5-IHN exhibits the highest percentage of heat loss among the configurations, implying that a larger portion of the generated heat is being dissipated through exhaust gases, coolant, and radiation rather than being converted into mechanical output. This increased heat loss in the 5-IHN setup may be attributed to over-atomization or suboptimal spray characteristics, which could lead to less efficient combustion despite greater fuel delivery.

A critical aspect examined in the study is the EGT, which is notably higher for the 4-IHN across all load conditions and biodiesel blend ratios. This elevated EGT is a key factor contributing to increased NOx emissions, highlighting a potential correlation between injector hole configuration and NOx formation. The enhanced combustion intensity associated with the 4-IHN likely leads to higher in-cylinder temperatures, which favor thermal NOx production.

Furthermore, the trend of rising EGT with increasing biodiesel blending ratios adds another layer of complexity, indicating that the chemical and physical properties of biodiesel, such as oxygen content and viscosity, can significantly influence combustion dynamics and emission behavior. This underscores the intricate relationship between fuel composition, injector design, and emission characteristics, emphasizing the need for optimized configurations when integrating biodiesel into existing engine systems.

The distinct properties of biodiesel—particularly its oxygenated structure and near carbon-neutral profile—play a significant role in influencing emission characteristics. While the use of biodiesel leads to a reduction in CO and CO₂ emissions due to more complete and cleaner combustion, it also results in paradoxically higher exhaust gas temperatures compared to conventional diesel. These elevated temperatures, especially when paired with certain injector configurations, contribute to increased NOx emissions, as higher combustion temperatures favor thermal NOx formation.

This nuanced interplay between biodiesel's physical-chemical properties, injector hole number, and resulting emission behavior highlights the complexity of optimizing engine performance while minimizing environmental impacts. Based on the findings, the study concludes that utilizing a 3-IHN in conjunction with biodiesel blends offers a promising balance, enhancing engine efficiency and reducing specific emissions, particularly CO and CO₂, without excessively elevating NOx levels.

5. CONCLUSION

Biodiesel has a lower calorific value and higher viscosity than diesel. So, it is preferred to use the blends of biodiesel in diesel engines. This research focused on assessing the heat conversion rates of biodiesel blends in diesel engines, with a specific emphasis on varying injector hole numbers. The thermal balance sheet, along with an analysis of emission characteristics, yielded valuable insights:

- ➤ Thermal Efficiency: The 3-IHN demonstrated superior heat-to-brake power conversion, achieving peak HBP values of 26.01% for the 5 JB blend at 70% load, outperforming both 4-IHN (20.20% HBP for diesel) and 5-IHN (17.81% HBP for diesel) configurations. This underscores the critical role of injector geometry in optimizing fuel atomization and combustion efficiency.
- ➤ Heat Dissipation: JB blends exhibited 8-15% lower HRad compared to diesel across all injector designs, highlighting their potential for improved thermal retention. However, 4-IHN and 5-IHN experienced significant radiative dissipation (up to 55.22% HRad), reducing usable energy output.
- ➤ EGT: The 3-IHN exhibited the lowest EGT at 261.07°C for 5 JB under full load, whereas the 5-IHN configurations produced significantly higher temperatures at 471.94°C

- for 5 JB, which directly correlates to a 31.32% increase in NO emissions for 20 JB blends.
- ➤ Emissions Profile: Increased injector hole numbers intensified CO, CO₂, and NO emissions, with 5-IHN yielding the most significant increases (19.28% higher CO for 20 JB). In contrast, biodiesel blends decreased CO and CO₂ emissions by 13.25-19.28% compared to diesel, due to their oxygenated molecular structure and higher cetane number.

These findings underscore the potential advantages of utilizing biodiesel blends, particularly those derived from Jatropha, in diesel engines with careful consideration of injector hole configurations for optimized thermal efficiency and reduced emissions.

ACKNOWLEDGMENT

We convey our heartfelt gratitude to the Thapathali Campus for providing the required platform for this project work. We express our sincere thanks to the Nepal Academy of Science and Technology (NAST), Nepal for the necessary lab work.

REFERENCES

- [1] Milton, B.E. (1998). Control technologies in sparkignition engines. Handbook of Air Pollution from Internal Combustion Engines, pp. 189-258. https://doi.org/10.1016/b978-012639855-7/50047-8
- [2] Sayin, C., Gumus, M., Canakci, M. (2013). Influence of injector hole number on the performance and emissions of a di diesel engine fueled with biodiesel-diesel fuel blends. Applied Thermal Engineering, 61(2): 121-128. https://doi.org/10.1016/j.applthermaleng.2013.07.038
- [3] Algayyim, S.J.M., Wandel, A.P., Yusaf, T. (2018). The impact of injector hole diameter on spray behaviour for butanol-diesel blends. Energies, 11(5): 1298. https://doi.org/10.3390/en11051298
- [4] Yoon, S., Lee, S., Kwon, H., Lee, J., Park, S. (2018). Effects of the swirl ratio and injector hole number on the combustion and emission characteristics of a light duty diesel engine. Applied Thermal Engineering, 142: 68-78. https://doi.org/10.1016/j.applthermaleng.2018.06.076
- [5] So Khuong, L., Hashimoto, N., Fujita, O. (2024). Spray, droplet evaporation, combustion, and emission characteristics of future transport fuels for compressionignition engines: A review. Journal of Traffic and Transportation Engineering, 11(4): 575-613. https://doi.org/10.1016/j.jtte.2024.04.003
- [6] Yadav, M., Yadav, A.K., Ahmad, A. (2025). Enhancing combustion and emission characteristics of CI engines through atomization and fuel—air mixing using non-circular orifices: A path towards sustainable biodiesel utilization. Green Technologies and Sustainability, 3(3): 100161. https://doi.org/10.1016/j.grets.2024.100161
- [7] Lee, B.H., Song, J.H., Chang, Y.J., Jeon, C.H. (2010). Effect of the number of fuel injector holes on characteristics of combustion and emissions in a diesel engine. International Journal of Automotive Technology, 11(6): 783-791. https://doi.org/10.1007/s12239-010-0093-2
- [8] Rajpara, P., Shah, R., Banerjee, J. (2022). Performance evaluation of upward swirl combustor with reverse fuel

- injector and hydrogen blending. Advances in Energy and Combustion, pp. 383-410. https://doi.org/10.1007/978-981-16-2648-7_17
- [9] Montgomery, D.T., Chan, M., Chang, C.T., Farrell, P.V., Reitz, R.D. (1996). Effect of injector nozzle hole size and number on spray characteristics and the performance of a heavy duty D.I. diesel engine. SAE Technical Paper 962002. https://doi.org/10.4271/962002
- [10] Mohiuddin, K., Kwon, H., Choi, M., Park, S. (2021). Experimental investigation on the effect of injector hole number on engine performance and particle number emissions in a light-duty diesel engine. International Journal of Engine Research, 22(8): 2689-2708. https://doi.org/10.1177/1468087420934605
- [11] Dong, S.J., Yang, C., Ou, B., Lu, H.G., Cheng, X.B. (2018). Experimental investigation on the effects of nozzle-hole number on combustion and emission characteristics of ethanol/diesel dual-fuel engine. Fuel, 217: 1-10. https://doi.org/10.1016/j.fuel.2017.12.024
- [12] Chauhan, B.S., Kumar, N., Cho, H.M. (2010). Performance and emission studies on an agriculture engine on neat Jatropha oil. Journal of Mechanical Science and Technology, 24(2): 529-535. https://doi.org/10.1007/s12206-010-0101-5
- [13] Forson, F.K., Oduro, E.K., Hammond-Donkoh, E. (2004). Performance of jatropha oil blends in a diesel engine. Renewable Energy, 29(7): 1135-1145. https://doi.org/10.1016/j.renene.2003.11.002
- [14] Akintayo, E.T. (2004). Characteristics and composition of Parkia biglobbossa and Jatropha curcas oils and cakes. Bioresource Technology, 92(3): 307-310. https://doi.org/10.1016/S0960-8524(03)00197-4
- [15] Agarwal, D., Agarwal, A.K. (2007). Performance and emissions characteristics of Jatropha oil (preheated and blends) in a direct injection compression ignition engine. Applied Thermal Engineering, 27(13): 2314-2323. https://doi.org/10.1016/j.applthermaleng.2007.01.009
- [16] Chauhan, B.S., Kumar, N., Cho, H.M. (2012). A study on the performance and emission of a diesel engine fueled with Jatropha biodiesel oil and its blends. Energy, 37(1): 616-622. https://doi.org/10.1016/j.energy.2011.10.043

- [17] Mofijur, M., Masjuki, H.H., Kalam, M.A., Atabani, A.E. (2013). Evaluation of biodiesel blending, engine performance and emissions characteristics of Jatropha curcas methyl ester: Malaysian perspective. Energy, 55: 879-887. https://doi.org/10.1016/j.energy.2013.02.059
- [18] Bhatta, K.R., Karna, R.L., Jha, A.K., Adhikari, S.P. (2021). Performance and emission characteristics of jatropha biodiesel blends in a direct injection CI engine. Himalayan Journal of Applied Science and Engineering, 2(2): 24-33. https://doi.org/10.3126/hijase.v2i2.43393
- [19] Palash, S.M., Kalam, M.A., Masjuki, H.H., Arbab, M.I., Masum, B.M., Sanjid, A. (2014). Impacts of NOx reducing antioxidant additive on performance and emissions of a multi-cylinder diesel engine fueled with Jatropha biodiesel blends. Energy Conversion and Management, 77: 577-585. https://doi.org/10.1016/j.enconman.2013.10.016
- [20] Wan Osman, W.N.A., Rosli, M.H., Mazli, W.N.A., Samsuri, S. (2024). Comparative review of biodiesel production and purification. Carbon Capture Science & Technology, 13: 100264. https://doi.org/10.1016/j.ccst.2024.100264
- [21] Datta, A., Palit, S., Mandal, B.K. (2014). An experimental study on the performance and emission characteristics of a CI engine fuelled with Jatropha biodiesel and its blends with diesel. Journal of Mechanical Science and Technology, 28(5): 1961-1966. https://doi.org/10.1007/s12206-014-0344-7
- [22] Liu, Z.Q., Bai, S.Q., Wang, J.L., Feng, S.Q. (2024). Effect of fuel injection parameters on the performance of a biodiesel engine. In Proceedings SPIE 13159, Eighth International Conference on Energy System, Electricity, and Power (ESEP 2023), 131593D. https://doi.org/10.1117/12.3024499
- [23] Zareei, J., Prasad, K.D.V., Kareem, A.K., Chandra, S., Shavkatov, N., Rodriguez-Benites, C., Guerrero, J.W.G., Ghazaly, N.M., Akhmetshin, E.M. (2024). Optimizing diesel engine performance and emissions with diesel-hydrogen mixtures: Impact of injector configuration, angle, and pressure. Energy Conversion and Management: X, 23: 100678. https://doi.org/10.1016/j.ecmx.2024.100678